

PHOTOPRODUCTION OF VECTOR MESONS AND
OTHER RESONANCES AT 4.3 BeV

by

Y. Eisenberg, B. Haber, Z. Carmel, E. Peleg, E. E. Ronat,
A. Shapira, G. Vishinsky, R. Yaari and G. Yekutieli

Department of Nuclear Physics
Weizmann Institute of Science, Rehovot, Israel

ABSTRACT

The SLAC 40" HBC was exposed to a 4.3 BeV positron annihilation radiation. Results are presented on reactions containing no neutrals and one neutral particle in the final state. For $\gamma p \rightarrow \rho^0 p$ and $\omega^0 p$ we find cross sections of $(19.2 \pm 1.2)\mu\text{b}$ and $(2.8 \pm .5)\mu\text{b}$ respectively. Assuming Vector Dominance, we determine the $V^0 p$ cross sections. Evidence for other resonant states is presented, in particular $\Delta^{++} V^0 \pi^-$, where we find $\Delta^{++} \rho^0 \pi^- / \Delta^{++} \omega^0 \pi^-$ about 1.5.

February 13, 1969

Previous studies of the photoproduction of multibody final states in bubble chambers were done by using a bremsstrahlung beam.^{1,2} In these studies no cross sections could be given for reactions having a neutral particle in the final state, except for some special cases such as ω^0 production. Recently, in order to overcome this difficulty, an e^+ annihilation photon beam was constructed at the Stanford Linear Accelerator Center (SLAC) by the SLAC Group.³ Some results of the SLAC Group at photon energies of 5.2 and 7.5 BeV were already published.³ In the present experiment we report on cross sections and resonance production at 4.3 BeV. The SLAC 40" hydrogen bubble chamber was exposed to a 4.3 BeV photon beam, obtained by the annihilation of an 8.5 BeV/c ($\pm 0.5\%$) e^+ beam in a liquid H_2 target. The beam details are given in Ref. 3. A total of 400,000 pictures were taken and the present results are based upon the analysis of about half the pictures. 5200 nuclear interactions, containing three or more prongs (or one prong, plus a V^0) were found in the above sample. We estimate that about one half of all our observed nuclear events are due to the monochromatic photons resulting from the e^+ annihilation. Since the energy of the monochromatic photons was known rather well (to within $\pm 2.5\%$), the kinematical analysis was similar to the usual one used for charged particle beams.

A summary of the reactions (1) - (6) studied so far and the cross sections obtained is given in Table I. For reaction (1), σ_T agrees with previous determinations.^{1,2} For reactions (2), (3), (5), and (6) σ_T has not been measured before at 4.3 BeV. The photon flux was monitored by measuring pairs every 100 picutres. A total of about 12,000 pairs were measured. In the present sample our event flux at 4.3 BeV was about 20 events/ μb . In all channels listed in Table I the separation between the monochromatic and bremsstrahlung events was very good. After ionization examination of all events, no events of reaction

(1) were ambiguous, while 10% of reactions (2) and 20% of reaction (3) remained ambiguous.

Photoproduction of ρ^0 p

The dominant channel in reaction (1) is the photoproduction of ρ^0 mesons ($\sim 80\%$), as can be seen from Fig. 1a, where the $\pi^+\pi^-$ invariant mass is plotted for the monochromatic events. A fit of the data to Jackson-type Breit-Wigner resonances was rather poor ($P(\chi^2) = .2\%$). However, with a Ross-Stodolsky⁴ mass dependent term ($\sim [M(\rho^0)/M(\pi^+\pi^-)]^4$) we obtain a very good fit ($P(\chi^2) = 85\%$). Similar results were obtained at DESY.² The ρ^0 central mass and width from this fit are: $M(\rho^0) = (760 \pm 5) \text{ MeV}$, $\Gamma = (136 \pm 12) \text{ MeV}$.

The ρ^0 production angular distribution, $d\sigma/dt'$ is shown in Fig. 1b. t' is $|t - t_{\min}|$, where t is the 4-momentum transfer between the photon and the ρ^0 , and t_{\min} is the minimum momentum transfer for each given $\pi^+\pi^-$ mass. For small $M(\pi^+\pi^-)$, and in the ρ^0 region, t_{\min} is essentially zero and thus $t' \approx t$. It is clear from Fig. 1b, that most of our data (up to $t' \approx .6 (\text{BeV}/c)^2$) could be well fitted to a curve of the type:

$$\frac{d\sigma}{dt'} = A \cdot e^{-Bt'} \quad (7)$$

The drop in the first 2 bins is not considered to be a real physical effect and is probably due to a low scanning efficiency for events with invisible or very short proton recoil in the bubble chamber ($R_p < 9 \text{ mm}$). Indeed, in the counter experiments,⁵ no such drop was observed. A best fit to Eq. (7) (for $t' = .05 - .6 (\text{BeV}/c)^2$) gives: $A = (145 \pm 15) \mu\text{b} (\text{BeV}/c)^{-2}$; $B = (7.6 \pm .5) (\text{BeV}/c)^{-2}$. These values are in good agreement with previous results.^{1,2,5,6} In the Vector Dominance Model (VDM)⁷ the photon is assumed to be coupled directly to the vector mesons (ρ^0 , ω^0 , ϕ^0) and thus the main contribution to ρ^0 photoproduction will come from elastic (diffractive) ρ^0 p scattering and we can write:

$$\frac{d\sigma}{dt} (\gamma p \rightarrow \rho^0 p) = C_\rho \cdot \frac{d\sigma}{dt} (\rho^0 p \rightarrow \rho^0 p). \quad (8)$$

$$C_\rho = \frac{\alpha\pi}{\gamma_\rho^2} = \frac{1}{4 \times 137} \times \left(\frac{\gamma_\rho^2}{4\pi} \right)^{-1} \quad \text{is usually assumed to be a constant and}$$

and not to depend upon t (we use the notations of Ref. 7). Using the recent Orsay value⁷ $\frac{\gamma_\rho^2}{4\pi} = .52 \pm .05$ we get $C_\rho = 3.5 \times 10^{-3}$. Parameterizing the elastic $\rho^0 p$ scattering in terms of a diffractive scattering of a sphere of radius R and transparency ϵ we have:

$$R^2 = 4B, \quad \alpha_T^{e1} = \pi R^2 (1 - \epsilon)^2, \quad \alpha_T^{e1} / \alpha_T = \frac{1}{2} (1 - \epsilon). \quad (9)$$

Further, from the optical theorem, assuming the forward scattering to be pure imaginary (diffractive) we have:

$$\frac{\alpha_T^2}{16\pi} = \left. \frac{d\sigma^{e1}}{dt} \right|_{t=0} \quad (10)$$

With $C_\rho = 3.5 \times 10^{-3}$, we obtain from our data and Eqs. (7), (8), (9), (10):

$$\sigma_T^{e1}(\rho^0 p \rightarrow \rho^0 p) = (5.5 \pm .5) \text{mb}, \quad \alpha_T(\rho^0 p) = (29 \pm 2) \text{mb}$$

$$R = (1.1 \pm .05) \text{fermi}, \quad \epsilon = .62 \pm .04.$$

These values are in agreement with $\alpha_T(\rho^0 p)$ determinations⁷ in photoproduction experiments on complex nuclei and are similar to the parameters derived from $\pi^\pm p$ scattering data.⁸ Thus we conclude that, within the framework of VDM, for $\rho^0 p$ scattering (as for pions), consistency of the slope of the forward diffraction peak and the magnitude of $d\sigma/dt$ at $t=0$ require a large transparency. One should note that using the value $\frac{\gamma_\rho^2}{4\pi} = 1.1 \pm .2$, as determined by the Cornell and SLAC⁵ experiments on the photo- ρ^0 production in complex nuclei, and our measured forward hydrogen cross section of $(145 \pm 15) \mu\text{b} (\text{BeV}/c)^{-2}$, we would obtain $\alpha_T(\rho^0 p) = (42 \pm 5) \text{mb}$. Taking $\alpha_T(\rho^0 p)$ to be⁵ $(30 \pm 5) \text{mb}$ and $\frac{\gamma_\rho^2}{4\pi} = 1.1$ would require the forward hydrogen cross section to be only $(75 \pm 25) \mu\text{b} (\text{BeV}/c)^{-2}$.

The slope B of the forward diffraction peak ($t' = 0 - .5 (\text{BeV}/c)^2$) decreases smoothly with increase of $M(\pi^+ \pi^-)$ (see also Ref. 2). A similar smooth decrease is

also observed when we plot B as a function of $M(\pi^+\pi^-\pi^0)$ in reaction (2): B is about 8 for M in the region .6 - .8 BeV and drops to $\sim 1-2$ (BeV/c)⁻² for masses around 2 BeV. A similar behaviour was recently reported in charged particle reactions⁹: while the mass plot shows many peaks, B as a function of M is smoothly decreasing. As far as we know, the origin of this effect is still not understood.

The ρ^0 decay density matrix elements, for the helicity system, are shown in Fig. 1c, as function of the ρ^0 production angle ($\cos \theta_{\text{c.m.}}$). For any simple diffraction model, including only spin independent interaction, (like the one described above, or the Strong Absorption Model, SAM),¹⁰ the density matrix elements in the Adair and helicity frames assume a particularly simple form:

$$\rho_{0,0}^A = \rho_{1,-1}^A = \text{Re } \rho_{1,0}^A = 0, \quad \rho_{0,0}^H = \frac{1}{2} \sin^2 \theta_{\text{c.m.}}, \quad \rho_{1,-1}^H = \frac{1}{4} \sin^2 \theta_{\text{c.m.}},$$

$\text{Re } \rho_{1,0}^H = -\frac{1}{\sqrt{32}} \sin 2\theta_{\text{c.m.}}$. The agreement of our data (Fig. 1c) as well as other experiments^{1,2,6,10} with these simple predictions is not bad in general.

More data, especially at higher t, are required for the definite determination of the importance of spin flip terms.

Photoproduction of ω^0 p

The invariant mass plot of the $\pi^+\pi^-\pi^0$ combination in reaction (2) is shown in Fig. 1d. A fit to a gaussian shaped ω^0 and phase-space yields $M(\omega^0) = (786 \pm 5)$ MeV and (experimental) width of 40 MeV. The ω^0 production angular distribution is shown in Fig. 1e. Again, some experimental loss of ω^0 events in the forward direction is evident. $\alpha_T(\omega^0)$ given in Table I has been corrected for this loss as well as for the ω^0 neutral decay mode (10%). A fit of the corrected data to a form $d\sigma/dt' = A e^{-Bt'}$ (constrained to give the total cross section, $A/B = (2.8 \pm .5) \mu\text{b}$) yields: $A = (20.5 \pm 4.5) \mu\text{b} (\text{BeV}/\text{c})^{-2}$, $B = (7.4 \pm 1.2) (\text{BeV}/\text{c})^{-2}$. The results are in essential agreement with previous data.^{1,2,6}

The interpretation of the ω^0 data is more difficult, since: (1) we have less events (by almost an order of magnitude) and (2) the ω^0 production mechanism is no longer pure diffraction and contains One-Pion-Exchange (OPE) contribution^{1,2} (at our energies). Thus, we have adopted the following approach. In analogy with Eq. (8), within VDM the diffractive part of ω^0 photoproduction can be written as:

$$\frac{d\sigma}{dt} (\gamma p \rightarrow \omega^0 p) = C_\omega \frac{d\sigma}{dt} (\omega^0 p \rightarrow \omega^0 p) \quad (8')$$

From SU(3) theory and $\omega^0 \rightarrow \ell^+ \ell^-$ experiments⁷ we know that $C_\rho : C_\omega = 9 : 1$. Thus we get: $C_\omega = .39 \times 10^{-3}$. Further, from SU(3) and the usual $\omega^0 - \phi^0$ mixing we get⁷ $\Gamma_{\rho\pi\gamma} : \Gamma_{\omega\pi\gamma} = 1 : 9$, neglecting the $\phi\pi\gamma$ coupling. Since experimentally $\Gamma_{\omega\pi\gamma} \approx 1$ MeV, the OPE contribution to ω^0 photoproduction at 4.3 BeV is still significant whereas for ρ^0 it can be neglected. Thus, combining the diffractive part of ω^0 production (assumed to be 10% of the ρ^0) and the OPE contribution¹¹ (including absorption corrections) we get the theoretical predictions for $d\sigma/dt'$ (Fig. 1e) and the decay distribution (Fig. 1f). The agreement with experiment is good and we conclude that our data is consistent with the above model. A more critical test of the theory will require much more data, and will be performed at a later stage.

Subtracting the (calculated) OPE contribution ($1.2 \mu\text{b}$), we can estimate from our data, using Eq. (8') and (10), the $\omega^0 p$ cross sections. We get: $\sigma_T^{e1}(\omega^0 p \rightarrow \omega^0 p) = (4.1 \pm 1.4)\text{mb}$ and $\sigma_T(\omega^0 p) = (27.4 \pm 3.2)\text{mb}$. These are close to our $\rho^0 p$ cross sections determined above.

Photoproduction of Other Resonances

In addition to the dominant production of ρ^0 and ω^0 , several other resonances have been observed and their cross sections are given in Table I. They will be discussed here very briefly.

1) $\pi^- \Delta^{++}$: Both σ_T and $d\sigma/dt$ are in agreement with the recent counter experiments.¹² The Δ^{++} decay correlations, which could not be measured in the counter experiments, are shown in Fig. 2a (see also Ref. 1,2). They yield (for $|t| < .2 \text{ (GeV/c)}^2$): $\rho_{11}^{GJ} = .41 \pm .13$. The expected value from OPE is 0.35.² Our data are in better agreement with OPE than those of Ref. 2.

2) $f^0 p$ and $g^0 p$: A better fit to Fig. 1a is obtained if one assumes that the peaks at the f^0 and g^0 position are due to resonances and not phase-space fluctuations. However, our evidence for the photoproduction of these resonances is inconclusive as yet (in Ref. 2, the estimate for f^0 was $(.4 \pm .3) \mu b$). Our limits for f^0 and g^0 cross sections are given in Table I. Their production angular distribution is rather flat. The g^0 meson, being a $J^{PC} = 3^{--}$ particle (presumably), can be photoproduced by a Pomeron exchange. In such a case, its decay distribution in the Adair system, neglecting spin effects,¹⁰ should be like the spherical harmonic $|Y_{3,\pm 1}|^2$. This is shown in Fig. 2b and is not inconsistent with our (rather scarce) experimental data. Note that our ratio $\sigma(g^0 p)/\sigma(\rho^0 p)$, which is $\sim 5\%$, agrees with other cases of inelastic/elastic ratios of Pomeron exchange reactions.¹³

3) $\rho^- \Delta^{++}$: This is presumably¹ due to OPE. Substantial amounts of $\rho^- \Delta^{++}$ production, bigger than $\pi^- \Delta^{++}$, is still visible at our energies (see Fig. 2c, d and Table I). In $\rho^- \Delta^{++}$ production a good ρ^- mass fit is obtained without the Ross-Stodolsky⁴ factor. The result is: $M(\rho^-) = (775 \pm 15) \text{ MeV}$.

4) Resonances in the 5-Prong Events (Reactions 4-6): These reactions are much more complicated to analyse because of the high multiplicities. The outstanding resonances observed are (see Fig. 2e, f) Δ^{++} , ρ^0 and ω^0 (Table I). Some evidence for associated production of these resonances is seen in our data (see Fig. 2f and Table I). Our cross sections are more or less in agreement with

previous data,^{1,2} when available. It is interesting to note that in the reactions $\gamma p \rightarrow \Delta^{++} V^0 \pi^-$ the ratio ρ^0/ω^0 is about 1.5, contrary to a ratio of $\sim 9/1$ (explainable within VDM and SU(3)) for the diffractive part of the "elastic" reactions, $\gamma p \rightarrow \rho^0 p/\omega^0 p$. This may mean that exchanges other than Pomeron are responsible for the complex reactions.

It is a pleasure to acknowledge the cooperation of SLAC in performing this experiment and, in particular, we are indebted to J. Ballam for his sincere encouragement throughout the experiment. We are grateful to the many members of Group B, in particular G. Chadwick, Z. Guiragossian, D.W.G.S. Leith and G. Wolf, for their kind help. Special thanks are due to A. Levy for his invaluable help during the early stages of the experiment. We greatly appreciate the efforts of the SLAC 40" HBC crew under R. Watt, the accelerator and beam crews, and especially A. Kilert. We wish also to thank our scanners and programming team for their excellent work and H. Harari for many interesting discussions. The work was supported, in part, by the Volkswagen Foundation.

REFERENCES

1. Cambridge Bubble Chamber Collaboration, Phys. Rev. 146, 994 (1966); 155, 1468 (1967); 163, 1510 (1967); 169, 1081 (1968).
2. Aachen-Berlin-Bonn-Hamburg-Heidelberg-München Collaboration, Phys. Rev. 175, 1669 (1968); Phys. Letters 27B, 54 (1968).
3. J. Ballam et al., Phys. Rev. Letters 21, 1541, 1544 (1968); SLAC-PUB-530, (1968).
4. M. Ross and L. Stodolsky, Phys. Rev. 149, 1172 (1966).
5. L. J. Lanzerotti et al., Phys. Rev. 166, 1365, (1968); H. Blechschmidt et al., Nuovo Cimento 52A, 1348 (1967); W. G. Jones et al., Phys. Rev. Letters 21, 586 (1968); G. McClellan et al., Cornell preprint, August 1968; F. Bulos et al., SLAC-PUB-541 (1969).
6. M. Davier et al., Phys. Rev. Letters 21, 841 (1968); SLAC-PUB-503 (1968).
7. For references on VDM and values of the direct photon-vector meson couplings obtained by various methods, see H. Harari, Phys. Rev. 155, 1565 (1967); S.C.C. Ting, Proceedings of the 14th Conference on High Energy Physics (Vienna, 1968); J. E. Augustin et al., Phys. Letters 28B, 508 (1969).
8. See, for example, the analysis of $\pi^\pm p$ data by B. E. Y. Svensson, CERN Report 67-24 II (1967) and M. N. Focacci et al., CERN 66-18 (1966) (unpublished). For (4-20) BeV/c $\pi^\pm p$ they get $\epsilon = .6 - .65$.
9. Aachen-Berlin-CERN-London Collaboration, Phys. Letters 27B, 336 (1968); G. Cocconi, Nuovo Cimento 57A, 837 (1968).
10. Y. Eisenberg et al., Phys. Letters 22, 217, 223 (1966); G. Kramer, DESY 67/32.
11. K. Schilling and F. Storim, Nucl. Phys. B7, 559 (1968).
12. A. M. Boyarski et al., Phys. Rev. Letters 22, 148 (1969).
13. See, for example, M. N. Kreisler et al., Phys. Rev. Letters 16, 1217 (1966); A. Shapira et al., Phys. Rev. Letters 21, 1835 (1968).

FIGURE CAPTIONS

1. (a) $M(\pi^+\pi^-)$ distribution for reaction (1). The solid curve represents best fit to ρ^0 , f^0 , g^0 resonances and phase-space. Dashed curve is phase-space alone. (b) Differential cross section $d\sigma/dt'$, for ρ^0 production ($M(\pi^+\pi^-) = .6 - .85$ BeV); curve is best fit to the shape $A e^{-Bt'}$, for the interval $t' = .05 - .6$ (BeV/c)². (c) The ρ^0 helicity density matrix elements in the ρ^0 rest frame, as a function of the c.m. production angle. Curves: predictions of SAM.¹⁰ (d) $M(\pi^+\pi^-\pi^0)$ distribution for reaction (2). The curve represents best fit to a gaussian shaped ω^0 and phase-space. (e) Observed $d\sigma/dt'$ for ω^0 production ($M(\pi^+\pi^-\pi^0) = (.74 - .82)$ BeV). The curve is the theoretical prediction (see text). (f) ω^0 decay distribution for the helicity system, $\cos\theta^H$, in the ω^0 rest frame. The curve: prediction of diffraction theory and OPE (see text).
2. (a) Decay distribution in the Gottfried-Jackson system ($\cos\theta^{GJ}$) of Δ^{++} ($M(p\pi^+) = 1.15 - 1.30$ BeV) produced in reaction (1). Curve is best fit to the data. (b) Adair system decay distribution ($\cos\theta^A$) of g^0 ($M(\pi^+\pi^-) = 1.5 - 1.8$ BeV) produced in reaction (1). Curve is expected distribution for diffraction production. Δ^{++} reflection (5 events) was removed. (c), (d) ρ^- and Δ^{++} production in reaction (2) (ω^0 events removed). Curves are best fits to resonances and phase-space. (c) $M(p\pi^+)$ distribution. Shaded area represents ρ^- region ($M(\pi^-\pi^0) = .65 - .85$ BeV). (d) $M(\pi^-\pi^0)$ distribution. Shaded area represents Δ^{++} region ($M(p\pi^+) = 1.15 - 1.35$ BeV). (e), (f) ω^0 and Δ^{++} production in reaction (5). Curves are best fits to resonances and phase-space, considering all possible self-reflections. (e) $M(p\pi^+)$ distribution. (f) $M(\pi^+\pi^-\pi^0)$ distribution. Shaded area represents Δ^{++} region.

TABLE I

Cross section for the 3 and 5 Prong Channels^(a) and Resonances at 4.3 GeV

	<u>Reaction</u>	<u>σ (μb)</u>	<u>Final State</u>	<u>σ (μb)</u>	<u>Final State</u>	<u>σ (μb)</u>
(1)	$\gamma\text{p} \rightarrow \text{p}\pi^+\pi^-$	$23.3 \pm 1.3^{(b)}$	$\rho^0\text{p}^{(b)}$	19.2 ± 1.2	$\pi^-\pi^0\Delta^{++}$	1.4 ± 1.1
(2)	$\rightarrow \text{p}\pi^+\pi^-\pi^0$	$21.6 \pm 1.4^{(b)}$	$f^0\text{p}$	$\leq .7 \pm .4$	$\pi^+2\pi^-\Delta^{++(d)}$	3.1 ± 1.1
(3)	$\rightarrow \text{n}\pi^+\pi^+\pi^-$	$12.1 \pm .9$	$g^0\text{p}$	$\leq .85 \pm .35$	$\rho^0\pi^+\pi^-\text{p}^{(d)}$	3.1 ± 1.1
(4)	$\rightarrow \text{p}2\pi^+2\pi^-$	$5.3 \pm .6$	$\pi^-\Delta^{++}$	$1.4 \pm .3$	$\pi^+2\pi^-\pi^0\Delta^{++(e)}$	$2.4 \pm .8$
(5)	$\rightarrow \text{p}2\pi^+2\pi^-\pi^0$	$7.0 \pm .7$	$\omega^0\text{p}^{(b,c)}$	$2.8 \pm .5$	$\omega^0\pi^+\pi^-\text{p}^{(c,e)}$	$1.6 \pm .5$
(6)	$\rightarrow \text{n}3\pi^+2\pi^-$	$3.9 \pm .5$	$\rho^-\Delta^{++}$	$3.2 \pm .8$	$A_1^0\pi^+\pi^-\text{p}$	$1.3 \pm .6$

(a) Ambiguous events were divided equally between the corresponding reactions.

(b) Corrected for loss in forward direction: $2.1 \mu\text{b}$ for ρ^0 and $0.4 \mu\text{b}$ for ω^0 .

(c) Corrected also for ω^0 neutral decay mode (10%).

(d) Of these, about $1.5 \mu\text{b}$ is associated production: $\Delta^{++}\rho^0\pi^-$.

(e) Of these, about $1 \mu\text{b}$ is associated production: $\Delta^{++}\omega^0\pi^-$. No ω^0 without Δ^{++} production (either in association or interfering with) is seen.

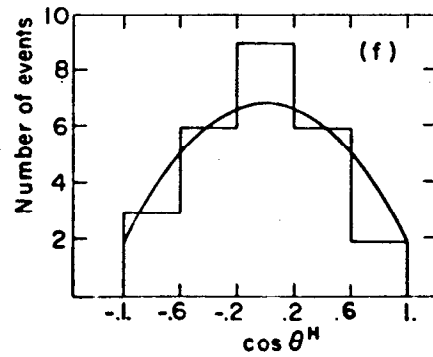
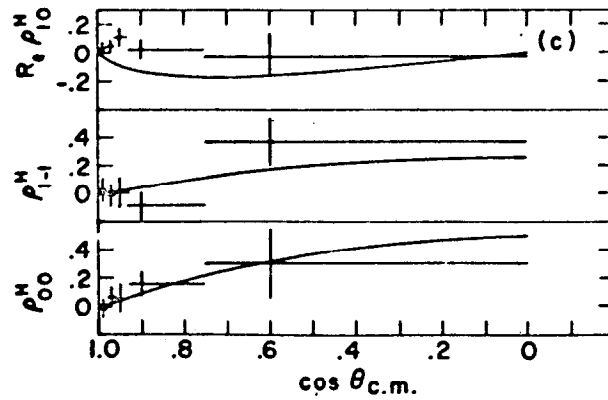
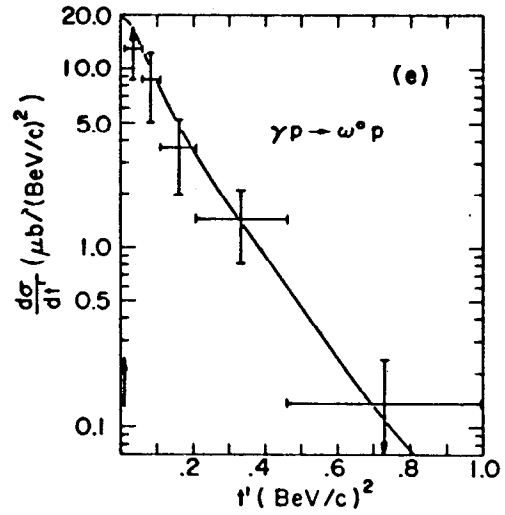
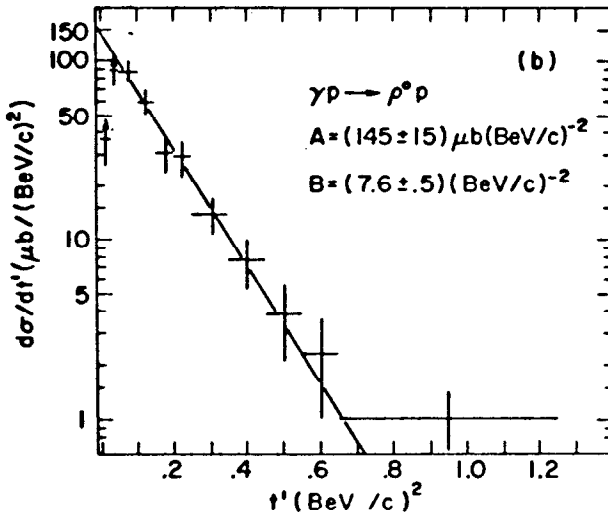
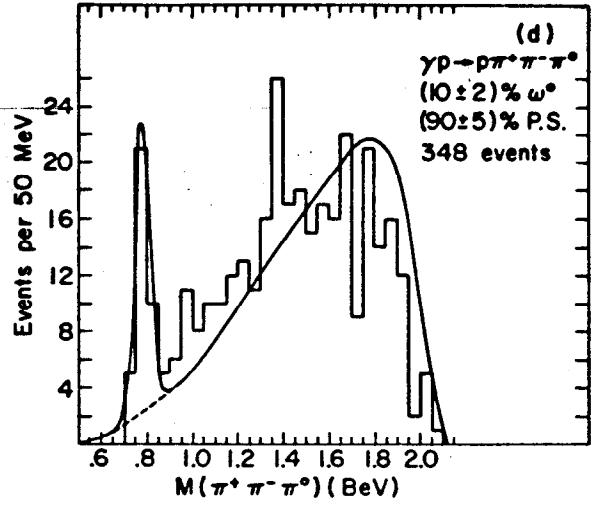
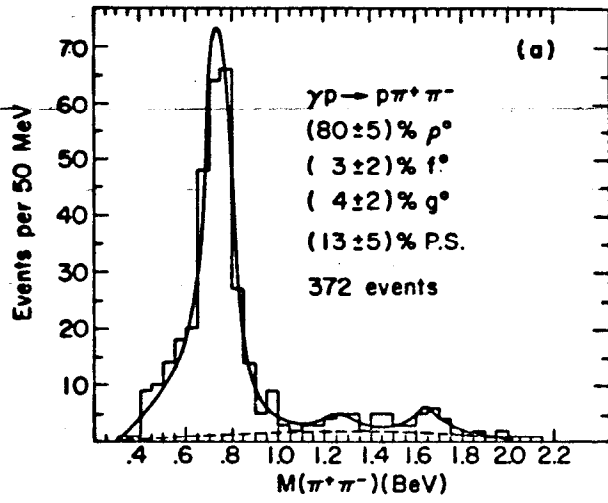


Fig. 1.

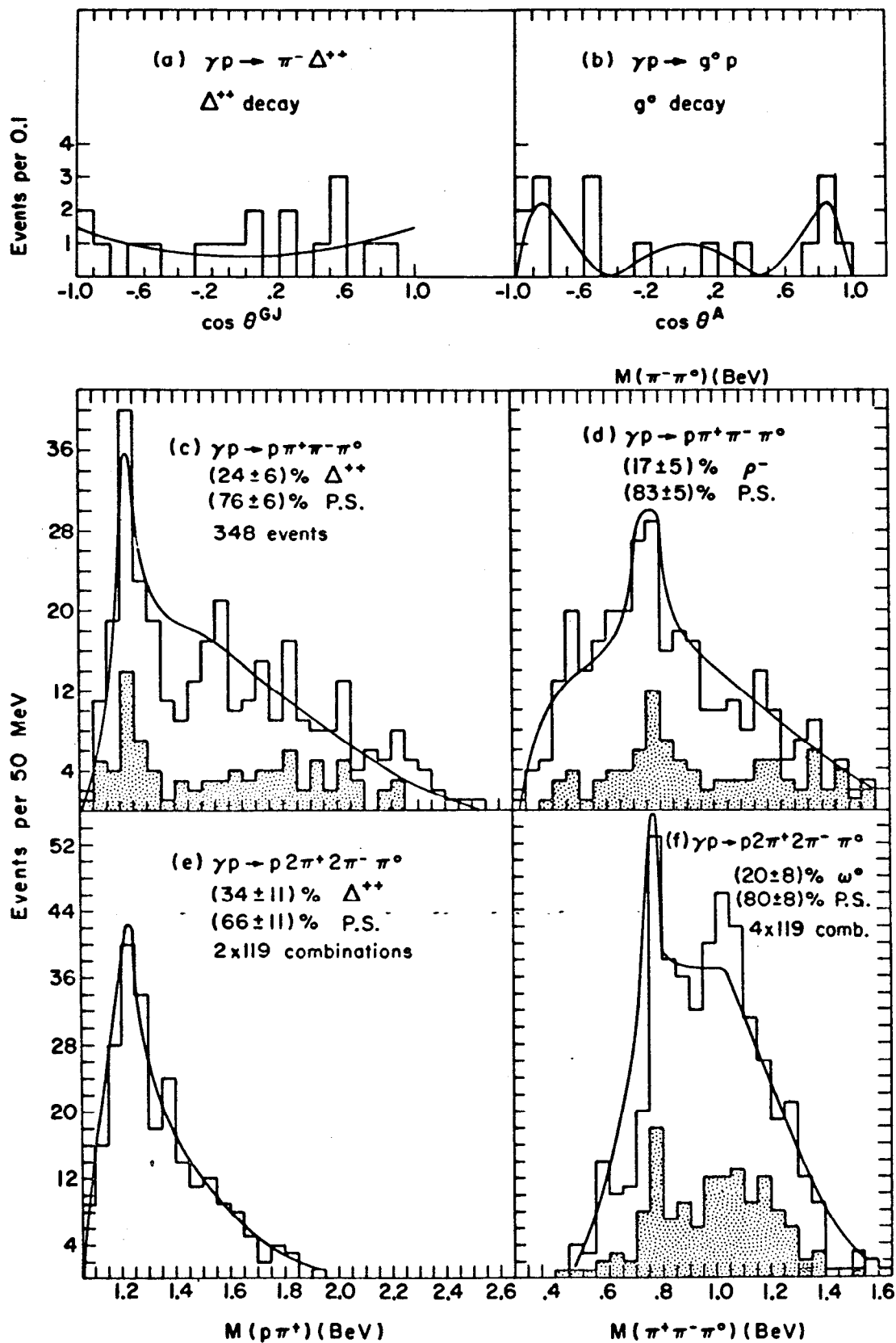


Fig. 2.